Journal of Bioenergetics and Biomembranes, Vol. 27, No. 3, 1995

Biological Electron Transfer

Christopher C. Moser,[1] Christopher C. Page,[1] Ramy Farid,[2] and P. Leslie Dutton[1]

Received April 11, 1995

Many oxidoreductases are constructed from (a) local sites of strongly coupled substrate–redox cofactor partners participating in exchange of electron pairs, (b) electron pair/single electron transducing redox centers, and (c) nonadiabatic, long-distance, single-electron tunneling between weakly coupled redox centers. The latter is the subject of an expanding experimental program that seeks to manipulate, test, and apply the parameters of theory. New results from the photosynthetic reaction center protein confirm that the electronic-tunneling medium appears relatively homogeneous, with any variances evident having no impact on function, and that control of intraprotein rates and directional specificity rests on a combination of distance, free energy, and reorganization energy. Interprotein electron transfer between cytochrome *c* and the reaction center and in lactate dehydrogenase, a typical oxidoreductase from yeast, are examined. Rates of interprotein electron transfer appear to follow intraprotein guidelines with the added essential provision of binding forces to bring the cofactors of the reacting proteins into proximity.

KEY WORDS: Intra-protein and inter-protein electron transfer; oxidoreductases; enzyme mechanisms.

INTRODUCTION: TYPES OF ELECTRON TRANSFER

Oxidoreductases were among the earliest enzymes to be recognized and have grown to be the biggest single group classified by IUPAC. One hundred years ago, oxidoreductase action was identified in yeast with the catalysis of fermentation. Today identification of oxidoreductase action continues to expand well beyond fermentative, respiratory, and photosynthetic energy metabolism. Redox cofactors in proteins are now appearing in many guises in the structures of a wide range of novel biological transformations that include nitrogen fixation, oxidative bursts in neutrophils, DNA repair, and in a growing number of signaling processes that govern gene regulation and expression (Padmanaban *et al.*, 1989; Edwards, 1994).

Numerically the class remains dominated by oxidations and reductions of otherwise stable substrates such as $NAD(P)^+/NAD(P)H$, water/dioxygen or many organic acid couples of intermediary metabolism. One of these is the lactate/pyruvate couple illustrated in Fig. 1 by lactate dehydrogenase from yeast (see Chapman *et al.*, 1991 for review). The essential stability of these and many other allied substrate-metabolites of intermediary metabolism and regulatory processes comes from the fact that their oxidation or reduction involves highly cooperative removal or insertion of two or more electrons. Often, electron transfer can only take place in pairs, frequently dressed as a hydrogen atom or hydride ion (Cha *et al.*, 1989), or with accompanying proton exchange with an aqueous phase. In Fig. 1, oxidation of lactate to pyruvate and reduction of flavin involves the breakage and formation of covalent bonds and transfer of two hydrogens. These classical enzymatic reactions, which are confined to a typical binding domain and involve the transfer of groups and atoms over fractions of an Ångstrom, represent the first major group of electron transfer reactions.

This manipulation of chemical bonds is an adiabatic reaction that follows the classical descriptions of

[1] The Johnson Research Foundation and Department of Biochemistry and Biophysics, University of Pennsylvania, Philadelphia, Pennsylvania 19104.

[2] Department of Chemistry, Rutgers University at Newark, Newark, New Jersey.

0145-479X/95/0600-0263$07.50/0

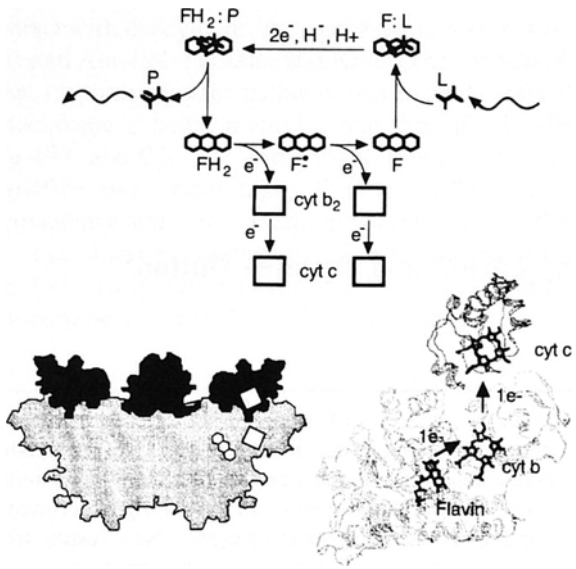

Fig. 1. Lactate dehydrogenase: a typical full-service oxidoreductase. Lactate dehydrogenase catalyzes the two-electron oxidation of lactate to pyruvate, using flavin as a transducer to deliver electrons singly to cytochrome *c* via heme *b*. At the top is a schematic representation of the chemical reaction starting with the adiabatic lactate binding, cooperative two-electron, two-hydrogen transfer to flavin, followed by release of pyruvate. Fully reduced flavin then participates in two sequential single electron reductions of cytochrome *b* and interprotein electron transfers to cytochrome *c*. At the bottom left is a side view of the outline of the tetrameric protein structure (light gray) as revealed by x-ray diffraction (Xia and Mathews, 1990), with the possible position of the four cytochrome *c* redox partners shown in darker gray (Tegoni *et al.*, 1993). These four cytochromes (two are essentially superimposed in the middle of the structure) are attracted to the negative charged region on the top of the tetramer. On the bottom right is a detail of one unit of the tetramer, with the structures of the flavin, heme *b*, and heme *c* darkened to illustrate the distance over which electrons are transferred.

molecular transformations that are the stuff of chemistry and biochemistry textbooks (Stryer, 1995; Voet and Voet, 1995). In the classical enzymological view, catalysis is achieved by stabilizing intermediate states and lowering transitional energy barriers to establish reaction rates that will support biochemical demand. At the same time, catalytic sites must have designed affinities for substrate and products to provide the required specificities for the reaction to operate in a crowded cell. The dynamics of the electron transfer itself can be readily obscured by the dynamics of binding as well as breaking and making bonds. Large-scale motions, such as redox partner diffusion and rotation, secondary binding, and protein conformation changes that are coupled to binding and redox changes at the catalytic sites can also obscure the transfer dynamics of the electron itself.

The adiabatic catalytic stages that are confined to the enzyme binding site in many of these substrate oxidoreductases are only part of the oxidoreductase action. The second major group of electron transfer reactions involves the molecular machinery to accept the multiple electrons and/or hydrogens or protons from the substrate and parley them into a currency of single-electron transfers and protolytic reactions. In the example of Fig. 1, flavin acts as a transducer by cycling between three stable redox states. After the cooperative electron-pair, two-proton reaction described above, the flavin then participates in two sequential one-electron transfers to the heme, cytochrome b_2, of the dehydrogenase. After protons are released and one electron is delivered to the heme, the flavin exists in a stable semiquinone state. Next, reduced heme b_2 is reoxidized by another heme, the external single electron carrier cytochrome *c*. To complete the cycle, the flavin semiquinone rereduces the heme b_2 again, and then itself becomes available for another cycle of catalysis. In oxidoreductases that reside in membranes, the counterpart to the flavin is the membrane-soluble cofactor ubiquinone that performs an analogous transducing function.

Many substrate oxidoreductases accommodate additional steps that involve electron transfer only. This third major group of electron transfer reactions confers on the oxidoreductase the capability to move electrons to and from the catalytic site over large distances, linking the catalytic site to some other part of the protein structure, perhaps to a remote binding site for another redox protein or perhaps to another catalytic site of substrate oxidation/reduction. In Fig. 1, oxidized cytochrome *c* previously bound to the surface of lactate dehydrogenase will engage in a long-range, single-electron transfer reaction. In the long-range electron transfers between sites, electrons are necessarily transferred as single entities through one or more intervening redox cofactors. Indeed in respiratory and photosynthetic systems, the catalytic sites of substrate oxidation and reduction and the electron pair/single electron interface are the gateways to extensive intervening single-electron transfer chains. These chains harness the redox potential free energy to transmembrane electrochemical gradients of protons that drive biosynthetic processes in cells (Mitchell, 1961).

In contrast to the first two major groups, long-range electron transfer reveals the control of a distinctly different set of forces. It has been known for

30 years that these strict electron transfers can be nonadiabatic in character and involve the quantum tunneling of the nuclei of the electron donor and acceptor and the atoms of surrounding protein and solvent as well as tunneling of the electron over long distance (Devault and Chance, 1966). In a biological context it is pertinent to regard long-range electron tunneling reactions that are nonadiabatic as remaining essentially enzymatic. The questions that are currently being posed in several laboratories regarding the enzymatic character of electron tunneling are focused on identifying what the factors are that govern the rate of transfer and confer directional specificity to the electron as it moves from one redox cofactor to another within a protein or from one protein to another. Electrons that go the wrong way can have devastating effects on the biological process, yielding a variety of debilitating pathologies in the short term and a range of age-related diseases in the long term (Ohnishi and Ohnishi, 1993).

PARAMETERS OF NONADIABATIC ELECTRON TRANSFER THEORY

The traditional enzymatic view of the chemical potential energy surface of an adiabatic reaction involves two energy minima, representing the reactant and product, with an intervening barrier. The height of the energy barrier, the activation energy, can be measured through the temperature dependence of the reaction. However, it is very difficult to estimate *a priori* what this activation energy will be based on the energy of the reactants and products. Even if extensive knowledge of the energy surfaces can be uncovered by experiment, extrapolation to other reactions is difficult (but see Warshel *et al.*, 1994).

The problem is often greatly simplified in nonadiabatic long-range electron transfer because the reactant and product surfaces are not strongly coupled (Devault, 1980). The Marcus theory is commonly used to describe the chemical potential energy surfaces and the free-energy dependence of these electron transfer reactions (Marcus, 1956; Marcus and Sutin, 1985). In this theory, reactants and products are modeled as two similar intersecting simple harmonic oscillator potentials. The potential minima are separated by an energy ΔG (the free energy of the reaction) and by a displacement of the atomic nuclei along the reaction coordinate. The reorganization energy, λ, is the amount of energy that must be added to the reactant at its potential minimum to bring the nuclei into the geometry resembling the product at its potential minimum without, however, transferring the electron. The point of intersection of the two potential surfaces is analogous to the transition state of an adiabatic reaction, with an activation energy

$$\Delta E\ddagger = (\Delta G + \lambda)^2/4\lambda \quad (1)$$

The rate of the electron transfer reaction has a simple Gaussian dependence on the free energy:

$$k \propto e^{-(\Delta G+\lambda)^2/4\lambda k_B T} \quad (2)$$

where k_B is the Boltzmann constant. There is an appealing simplicity of this model. A Gaussian dependence could be the result of many causes, not only because a simple harmonic oscillator model is a particularly good description. A Gaussian free-energy dependence of the rate has an important nonclassical enzymological result. The reaction rate is optimized when the free energy matches the reorganization energy. Overdriving the reaction results in a rate decrease, and defines the Marcus inverted region. The inverted region could be critical in large free-energy reactions, such as those found in light-activated photosynthetic systems or in the single-electron oxygen reduction/water oxidation steps of respiration, superoxide dismutase, catalyase, and peroxidase or P450.

The photosynthetic reaction centers provide an extensive laboratory for investigating intraprotein electron transfer. Light activation of the reaction center circumvents adiabatic reactions like substrate binding and coupled electron pair transfer reactions. Extraction and replacement of the quinone cofactor with exotic redox centers, as well as site-directed mutagenesis around the chlorins, has resulted in an unusually extensive rate vs. free-energy relationship for many of the physiologically productive charge separation and physiologically unproductive charge recombinations within the reaction center (see Fig. 2). The free-energy dependence of a number of these reactions appears to rise to a maximum and in some cases begins to decrease in a manner at least roughly described by a Marcus model. The reorganization energy seems to vary within a range of 0.5 to 1.2 eV for most reactions, depending upon the polarity of the protein environment around the redox centers. The 3-psec initial charge separation appears to have an unusually small reorganization energy of around 0.2 eV, together with small free-energy values (Warshel *et al.*, 1989; Parson *et al.*, 1990). In view of the accessibility of the inverted region for charge recombination to ground state in these early light-activated reactions, there seem to be good engineering reasons to make these steps have a

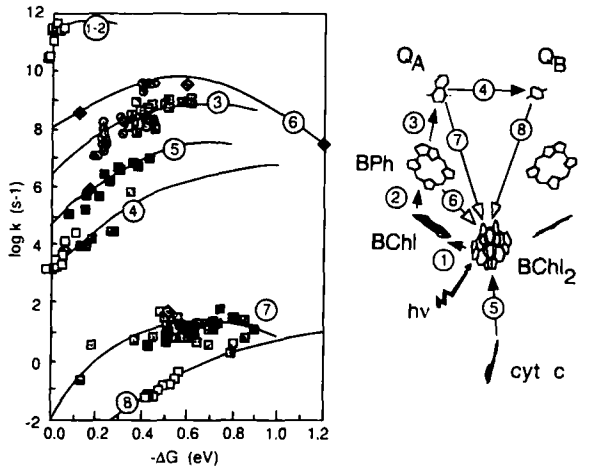

Fig. 2. The free-energy dependence of various electron-transfer reactions within the photosynthetic reaction center, as explored by quinone extraction and replacement (gray) and site-directed mutagenesis (black and white). Reaction are identified by number in the cofactor arrangement for *Rp. viridis* at the right. Productive charge-separating reactions are shown as filled arrows, unproductive charge recombinations as open arrows. Native rates are shown as diamonds or an ellipse. The initial charge is interpreted here as a two-step mechanism involving the intervening BChl monomer (Holzapfel *et al.*, 1990), although a single-step mechanism is possible, especially when site-directed mutants (white squares) (Jia *et al.*, 1993) are used to modify the native free energies. Quinone substitution describes a free-energy dependence for reaction 3 in *Rb. sphaeroides* (gray squares) (Gunner and Dutton, 1989) and *Rp. viridis* (gray circles) (Moser *et al.*, 1992). Quinone substitution was also performed for reaction 4 (gray squares) (Giangiacomo and Dutton, 1989), as was site-directed mutagenesis (white squares) (Okamura and Feher, 1992). Reaction 5 is explored by site-directed mutagenesis around the $BChl_2$ partner (black squares) (Lin *et al.*, 1994b). Reaction 6 is represented by only two native points (black diamonds) (Parson *et al.*, 1975; Holten *et al.*, 1978; Schenck *et al.*, 1982; Chidsey *et al.*, 1985; Shopes and Wraight, 1985), with the different free energies represented by singlet and triplet recombination rates. Reaction 6 is explored by both quinone substitution (gray squares) (Gunner *et al.*, 1986) and by site-directed mutagenesis around $BChl_2$ (black squares) (Lin *et al.*, 1994a). Reaction 7 is explored by site-directed mutagenesis (white squares) (Labahn *et al.*, 1994). Black curves are akin to the Marcus relationship, but include a quantum correction using a high-energy vibration (characteristic frequency) of 70 meV (Moser *et al.*, 1992).

small reorganization energy (Warshel and Weiss, 1978; Beitz and Miller, 1979; Moser and Dutton, 1992). Apparently, reorganization energy, expressed as the response of the protein environment to the electron transfer reaction, is subject to natural selection. On the other hand, we see no evidence for natural selection acting on the frequencies of nuclear motion coupled to electron transfer to adjust electron transfer rates (Moser *et al.*, 1992).

At very low temperatures where many tunneling electron transfers are still active, quantum mechanical terms cannot be ignored. There are a number of possible quantum approximations to choose from, such as partly (Hopfield, 1974; Jortner, 1976) or fully quantized description using a harmonic oscillator with a characteristic frequency (Levich and Dogonadze, 1959). It is not now clear how much quantum mechanical notation is needed to come up with sufficient accuracy to accommodate data which is full of experimental uncertainties. So far relatively simple expressions that prevent the narrowing of the Marcus Gaussian relationship at low temperatures seem to be sufficient (Gunner and Dutton, 1989; Moser *et al.*, 1992).

By comparing optimum electron transfer rates (when the free energy matches the reorganization energy), it is possible to mostly remove the nuclei-dependent, Franck–Condon terms and examine the dependence of the electron rate on the electronic coupling of reactant and product. The very weakness of the coupling of the potential surfaces of reactants and product in a nonadiabatic description means that the electronic coupling becomes a principal determinant of rate. Figure 3 illustrates that to a first approximation, electron transfer rates in photosynthetic reaction centers seem to scale exponentially with edge-to-edge distance over a vast range of magnitudes (Moser *et al.*, 1992). The natural base exponential decay coefficient defines $\beta = 1.4$ Å^{-1}. Simple theory suggests that tunneling through a relatively long, uniform barrier will fall exponentially with distance.

PARAMETERS NATURALLY SELECTED TO GOVERN REACTION RATES AND DIRECTIONAL SPECIFICITY

Taken together, the electronic coupling data from reaction centers suggests that there are three principal parameters which are subject to natural selection in determining intraprotein electron transfer rates: edge-to-edge distance, free energy, and reorganization energy. An empirically based room temperature rate expression (Moser and Dutton, 1992) which includes only these three principal parameters is

$$\log k_{et} = 15 - 0.6{*}R - 3.1(\Delta G + \lambda)^2/\lambda \quad (3)$$

where R is the edge-to-edge distance in Angstroms, and ΔG and λ are expressed in eV. This is a simple Gaussian dependence of electron transfer rate on free

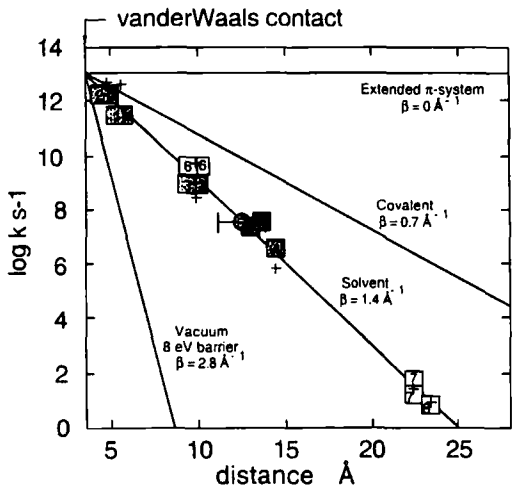

Fig. 3. The log of the free-energy-optimized rates of electron transfer in the photosynthetic reaction centers of *Rp. viridis* and *Rb. sphaeroides* follow a nearly linear dependence on distance. Free-energy-optimized rates are obtained from Fig. 2. Edge-to-edge distances are obtained from crystal structures (Chang *et al.*, 1986; Michel *et al.*, 1986; Allen *et al.*, 1987). Reactions are numbered as in Fig. 2. Physiologically productive rates are shown in gray squares. Physiologically counterproductive charge recombinations are shown as white squares. There is no evidence that the productive reactions are consistently faster than unproductive reactions at a given distance. Point 5′ represents the cytochrome *c*/reaction center complex from *Rb. sphaeroides* using a range of modeled distances (Allen *et al.*, 1987; Tiede and Dutton, 1993). Lines represent rate dependences based on uniform tunneling barriers of various heights and correspond to the beta values which reflect the natural log slope. Crosses represent electron transfer rates from a binary tunneling barrier approximation for *Rb. sphaeroides*.

energy and a simple exponential dependence on distance. Considering its simplicity and its few adjustable parameters, it is relatively successful as a first approximation to all the various electron transfer rates in reaction centers. Table I shows that the standard deviation between this simple relation and measurements of native electron transfer rates is about 0.4 log units or a factor of 2.4. These rate calculations use crystal structure distances for *Rb. sphaeroides* and *Rp. viridis* reaction centers, and experimental measurements of free energy and estimates of λ based on free-energy variation of the electron transfer rate. This empirical relation has the advantage of being easily applied to many systems to generate testable predictions.

Examining more closely just the electronic coupling, Fig. 3 shows that a β value for intraprotein electron transfer in reaction centers is intermediate between that experimentally apparent for covalently linked systems, and that estimated for a vacuum (Moser *et al.*, 1992). It appears that the electronic wavefunction propagates through a medium with an effective barrier height that varies between the relatively low covalent-like barrier found near atomic nuclei and the relatively high barrier height in those vacuum-like regions far from the nuclei. On the average, the barrier appears to be similar to that observed in frozen organic solvent (Miller *et al.*, 1984), at least for the reaction center.

Although the tunneling barrier presented to the electron by the amino acid environment in a protein has an extremely complicated spatial dependence, there are several reasons why a solvent-like (vs. covalent or vacuum-like) barrier may be a practical description in nearly all physiologically relevant long-distant electron transfer reactions.

First, unless there is a strong selection of the intervening protein medium to be more or less covalently linked, the tunneling properties of the medium between redox centers will tend to depend upon an apparently random assembly of amino acids and resemble the relatively "structureless" quality of an organic glass over distances that are large compared to the size of an amino acid.

Second, when natural selection operates on an existing enzyme, it does so principally by means of random mutations or deletions and insertions of amino acids, most of which must preserve the general function of the enzyme or be selected against. It may well be difficult to make significant structural changes that affect the tunneling barrier without at the same time compromising the assembly, stability, or other critical roles of the protein matrix. Despite our focus on the biological basis of electron transfer rates, we must avoid the chauvinism that amino acid selection can be understood principally in terms of these rates.

Third, even if flexible structural mutation is possible, it appears that there are more direct and accessible mutational means to modify electron transfer rates, for example by changing the polarity of amino acids immediately surrounding the cofactors to modify reaction free energy and reorganization energy.

Fourth, electron transfer reactions appear to be relatively simply and robustly engineered, such that the electron transfer rates for many individual reactions can vary considerably without affecting the overall function of the enzyme within the bioenergetic scheme, for example, in the effective interconversion of lactate and pyruvate in lactate dehydrogenase, or in the effective transmembrane charging, quinone reduction, and cytochrome *c* oxidation by the photosynthetic reaction center (Moser and Dutton, 1992). Thus, relatively

small changes in electron transfer rates that might result from medium structural changes may not be strongly selected for or against.

Fifth, biological redox centers tend to be relatively large compared to some of the metal centers that can be synthesized chemically. Since the electron is often significantly delocalized over native redox centers, the electron tunneling into the medium barrier in all directions will tend to sample relatively large regions of the protein between cofactors. This effect tends to minimize the importance of any one structural feature. For electron transfer between single atom redox centers, this structural averaging may not apply.

Sixth, electron transfer proteins are dynamic structures whose motions and structural heterogeneity will result in the electron sampling many protein microstates. For example, individual residues may turn, small molecules like water will move about to different positions, adjacent helices can slide or bend relative to one another, or proteins can suffer chemical modification during their useful lifetimes. In the extreme case, protein function may require the physical attraction, binding, and release of redox cofactors themselves, such as ubiquinone or cytochrome *c*. These changes will also tend to minimize the importance of any specific bond or gap geometry in the intervening medium in a particular microstate.

Apparently photosynthetic reaction centers *have not been selected* to covalently link redox centers in order to accelerate productive electron transfers and place numerous nonbonded gaps in unproductive, energetically wasteful, electron transfers. In most cases, it appears that setting the relative proximity of redox centers is the principal means to assure the productive sequence of intraprotein electron transfers.

If, as appears to be the case, the reaction center protein medium presents a similar barrier to electron tunneling for the electron transfers that are physiologically productive and unproductive, the burden for the strong directional specificity for an electron on the excited state bacteriochlorophyll dimer, $BChl_2$, to forward charge separation through the monomer BChl, and the BPh to Q_A across the membrane with only minor competing backward returns to the ground state, must rest on the Franck–Condon factors. For example, the much debated directional electron transfer from the excited state along the L- (or A-) branch and not the M- (or B-) branch of the approximately C2 symmetric reaction center is a situation where distances for alternate reactions are similar, and Franck–Condon factors depending on free energy and reorganization energy are likely to be important in determining the direction of electron transfer. In the simplest case, the M-branch BChl could present an unfavorable free energy of reduction relative to the L-branch BChl.

EFFECT OF PROTEIN STRUCTURE ON ELECTRONIC COUPLING

Despite the apparent success of a single solvent-like β in describing the electronic coupling in the reaction center, inspection of the structure of the reaction center and other protein structures suggests that substantial statistical variation of connectedness of protein medium between redox centers is possible. This variation might become large enough to become noticeable in some physiologically relevant reactions. For example, Q_A and Q_B are connected by histidines and a symmetrically placed Fe to form a structure analogous to some of the covalent systems. Structural effects on rates are more likely to be uncovered with the intentional chemical attachment of redox centers to well-chosen amino acids. Beginning with the first photoactive ruthenium coordination in cytochrome *c* (Pan *et al.*, 1988), such modifications of myoglobin, cytochrome *c*, and plastocyanin have allowed the experimental selection of structural regions or motifs which are deliberately more or less connected than average (Farver and Pecht, 1992; Willie et al., 1992; Wuttke *et al.*, 1992a,b; Casimiro *et al.*, 1993a,b; Karpishin *et al.*, 1994). Some ruthenium modified proteins have revealed rates larger or smaller than that expected for a solvent-like β of 1.4 $Å^{-1}$. An excellent example is provided by a ruthenated cytochrome b_5 (Willie *et al.*, 1992) in which the Ru and heme Fe are more or less directly linked by a covalent bridge. The rate observed in this reaction falls on the line $\beta = 0.7$ $Å^{-1}$ describing other covalently linked systems in Moser *et al.*, (1992), and well above the line describing native rates.

It is not clear how much sophistication in analyzing the connectedness is needed to accommodate the native and chemically modified data set (Farid *et al.*, 1993; Friesner and Monge, 1994). A computationally modest appraisal of the contribution of varying connectedness found in the protein medium can be found by looking at how much of the medium between the redox centers is relatively close or relatively far away from atomic nuclei. Because many biological redox centers are relatively large, it may be appropriate to look at the corridor between redox centers that is defined by the collection of lines of sights connecting each atom on the donor and acceptor that has signifi-

cant tunneling electron density. This elementary probe of protein structure may provide a formal means of estimating the natural variation of intraprotein electron transfer rate expected for a given distance, or the likely range of distances given a rate. Understanding the statistics of protein connectedness would make this approach useful even for oxidoreductases for which there is no resolved crystal structure.

A simple formalism begins with identifying the N atoms that make up the donor and the M atoms that make up the acceptor. We choose cofactor atoms which are likely to include appreciable tunneling electron density. For chlorins and porphyrins these are the atoms of the resonant macrocycle, excluding peripheral substituents but including any central metal atom and the immediate atom of each ligand. For quinones, we include the quinone ring and attached oxygens but exclude alkyl substituents such as the polyisoprene tail (Warncke *et al.*, 1994). We examine the line defined by each of the N × M donor–acceptor atom pairs and identify the lengths of lines that fall within 1.7 Å (an approximate Van der Waals radius) of any heavy atom center resolved by the PDB crystal structure. These lengths are assigned a β, for example 0.7 $Å^{-1}$, corresponding to the observed exponential decay of the rate of electron transfer with distance for rigid covalently linked systems (Moser *et al.*, 1992) and a tunneling barrier of about 0.5 eV. For the length of line further than 1.7 Å from a heavy atom center, typically 45% of the line, we choose a larger β of 2 $Å^{-1}$, corresponding to a higher tunneling barrier of about 4 eV. Using this binary barrier approximation we can then average the N × M rates for a single final value. This formalism naturally emphasizes the rate for the shortest edge-to-edge distance, but accommodates the variations in density of the medium from one region of the protein to another. Rates calculated by this approach (crosses in Fig. 3) deviate from a single barrier model by up to 8-fold. This deviation is comparable to the deviation of the experimentally based free-energy optimized rates of Fig. 3 and within the uncertainty of these estimates.

The approach just described is basically a one-dimensional approximation in which the tunneling barrier jumps repeatedly between two levels, one corresponding to a lower covalent-like barrier, and one to a higher vacuum-like barrier. Other barrier approximations have been described. A relatively simple model is based on a smoothly varying potential similar to the hydrogen molecule ion, H_2^+ (Devault, 1980). It is possible that when the tunneling barrier gets small enough, a complex distance dependence might be found (Evenson and Karplus, 1993).

Other approaches are explicitly three-dimensional. An artificial intelligence approach has been used to find relevant regions of the protein medium on which second-order perturbation theory is used to calculate electronic coupling elements (Siddarth and Marcus, 1993). Another technique uses Monte Carlo methods and a detailed barrier calculation (Kuki and

Table I. Distances, Free Energies, Reorganization Energies, and Calculated and Measured Electron Transfers in Native Photosynthetic Reaction Centers from *Rb. sphaeroides* and *Rp. viridis*[a]

Reaction	R(Å)	ΔG(eV)	λ(eV)	log k_{calc} (s^{-1})	log k_{obs} (s^{-1})	Deviation
			Charge separations			
P-B sph.	5.0	0.08	0.2	11.5	11.5	0.0
P-B vir.	5.5	0.08	0.2	11.5	11.5	0.0
B-H sph.	4.6	0.08	0.2	12.0	12.0	0.0
B-H vir.	4.8	0.08	0.2	11.9	12.0	−0.1
H-Qa sph.	10	0.60	0.7	9.0	8.7	0.3
H-Qa vir.	9.6	0.60	0.7	9.2	8.7	0.5
Qa-Qb sph.	14.5	0.07	1.0	3.6	4.0	−0.4
Qa-Qb vir.	13.5	0.07	1.0	4.2	4.0	0.2
			Recombinations			
1H-P sph.	10.1	1.20	0.6	7.1	7.5	−0.4
3H-P sph.	10.1	0.12	0.6	7.7	8.7	−1.0
Qa-P sph.	22.5	0.52	0.8	1.2	1.0	0.2
Qb-P sph.	23.4	0.45	1.2	−1.0	−1.2	0.2

[a] P: bacteriochlorophyl dimer; B: bacteriochlorophyl monomer; H: bacteriopheophytin; Qa, Qb: primary and secondary quinone. Value for λ for Qb-P from Labahn *et al.* (1994). See Moser *et al.* (1992) for other references.

Wolynes, 1987; Gruschus and Kuki, 1993). This approach suggests that a relatively large region of the protein medium between redox centers is relevant. For example, for a 15 Å electron transfer, an ellipsoid which includes 50% of the area of relevance to coupling has a 6.4 Å diameter, while the volume including 90% of the coupling is 11.8 Å in diameter. For a 20 Å electron transfer these diameters are 7.1 and 13.1 Å.

A different sort of algorithm (Beratan *et al.*, 1992; Betts *et al.*, 1992; Onuchic *et al.*, 1992) constructs electron transfer pathways from covalent linkages between adjacent atoms, hydrogen bonds, and through space jumps. Electronic coupling through such a pathway is a product of the coupling through each type of link. A simplifying approximation can be made that the coupling through all covalent bonds is approximately the same, that coupling through a hydrogen bond is comparable to that across approximately two covalent bonds, and that through space coupling is distance dependent. A search of the myriad pathways that connect a donor and acceptor leads to one or a small number of optimal pathways that have relatively few through space jumps. In a study of ruthenated derivatives of cytochrome *c*, where the ruthenated position is selected to accent either a particularly disconnected or covalently linked protein section, the pathway analysis correlates better with electron transfer rate than a single exponential dependence on distance (Karpishin *et al.*, 1994).

One of the problems of any calculation based on a published crystal structure is that such a structure does not include unresolved atoms, most obviously water molecules that can fit in the interstices between amino acids in one or more of a myriad of conformational substructures. Even with a new *Rb. sphaeroides* structure (Ermler *et al.*, 1994), which has defined many more water positions, the density of the published structure appears about 10% less than expected based on typical values for protein specific gravity. As a result, any wavefunction propagation models which rely on crystal structures and ignore the undefined waters can be misleading. Clearly some provision for these uncertain players in modulating the protein medium needs to be made. In the binary barrier approximation, additional water molecules may be one reason why the energy barrier for tunneling through protein regions without crystal structure heavy atoms appears as low as 4 eV. A related problem facing crystal structure-based calculations is the potentially variable position of the cofactors. This is a clear concern in *Rb. sphaeroides* in which the position of Q_B is clearly different in the newest structure (Ermler *et al.*, 1994) relative to the others. Indeed, the variable placement of reconstituted quinones may explain some of the rate variability found in Fig. 2 (Dutton and Moser, 1994). The variable placement of cytochrome *c* is also a concern in cytochrome complexes, such as the co-crystal structure of cytochrome *c* with cytochrome *c* peroxidase (Pelletier and Kraut, 1992; McLendon *et al.*, 1993).

Another fundamentally unavoidable problem faced by these relatively simple models is how to define the distance between redox centers. To put the problem another way, it is not entirely clear where a cofactor ends and the protein medium begins. One of the most obvious problems concerns hemes in which the redox center might reasonably be considered to be just the central Fe atom, or include the conjugated heme macrocycle. It appears that this concern can be addressed experimentally by looking at various heme–heme electron transfers in a variety of native electron transfer proteins with different heme–heme geometries.

Of course all of these models rely on a dependable data set (Friesner and Monge, 1994). Separating the electronic coupling from the Franck–Condon factors is essential for interprotein comparisons, but reliable rate vs. free energy profiles are difficult to achieve. Much progress has been made in single and double amino acid mutational changes in reaction free energy (see Fig. 2), but mutational changes can also introduce other modifications, for example in reorganization energy and structure, that can be problematic. Applied electric field changes of free energy may develop into a general and powerful technique (Franzen *et al.*, 1990; Volk *et al.*, 1993; Moser *et al.*, 1995).

PROTEIN STRUCTURE DESIGN FOR INTER-PROTEIN ELECTRON TRANSFER

The dramatic dependence of electron transfer rate on distance in the reaction center raises the question as to how the reaction center and other proteins might be designed for control of electron transfer in and out of the protein. A calculation analogous to the simple algorithm described above, but imagining the individual heavy atoms to be separate redox cofactors, generates a picture of the relative rate of electron tunneling at the surface of a protein. Figure 4 shows a view looking from the outside of the *Rb. sphaeroides* photosynthetic reaction center at the surface exposed to the

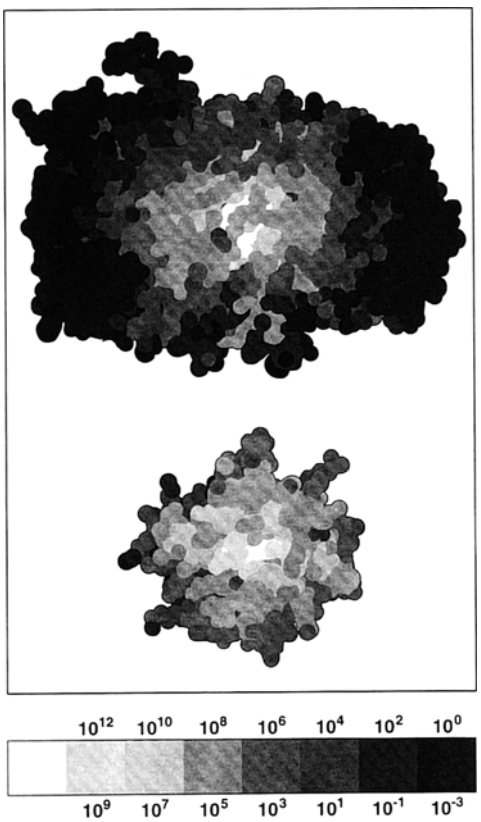

Fig. 4. The relative electron tunneling density of the bacteriochlorophyll dimer face of the photosynthetic reaction center from *Rb. sphaeroides* (top) and the heme face of cytochrome *c* (bottom), as calculated using a binary barrier approximation. Light areas indicate regions of relatively high tunneling electron density corresponding to regions in which electron transfer with a redox partner would be rapid. The scale at the bottom shows the electron transfer rates expected if each surface atom were a hypothetical redox partner, with the upper rates corresponding to a free-energy-optimized reaction ($-\Delta G = \lambda$) and the lower rates for a free energy of about 120 meV, similar to the native free energy for this reaction. The grays in the lighter half of the array define a relatively broad area in which contact between cytochrome *c* and reaction center would result in electron transfer rates supporting physiological function, in keeping with the soft binding view that several interprotein complex geometries are functionally active.

water of the cell's periplasm where interprotein electron transfer occurs between the reaction center $BChl_2$ and the cytochrome *c* heme. The edges of the $BChl_2$ macrocycles are partially visible from the surface. Also shown in Fig. 4 is a companion view of the heme face of cytochrome *c* where again the heme edge is visible in the cleft from the surface. The lightest areas represent a region of the protein where the tunneling density should be the greatest, with a rate decrease of 2 orders of magnitude for every deeper shade of gray. What is clearly apparent from these presentations is the large area on each protein that can be identified as regions of high tunneling density and hence endowed with the potential for rapid interprotein electron transfer. In contrast, the sides and back of the cytochrome *c* (not shown) are dominated by dark areas indicative of low electron tunneling density. Likewise on the reaction center surfaces there are no other regions accessible to the cytochrome that could support electron transfer rates of any biological significance.

The high tunneling density regions are likely to be essential features of the proteins designed to promote electron transfer between the cytochrome heme and the $BChl_2$ of the reaction center; however, a recent detailed study into the nature of the interaction between the reaction center and various cytochromes *c* has emphasized that while proximity is necessary, it is far from sufficient. Tiede and Dutton (1993) and Tiede *et al.* (1993) have demonstrated that without significant binding affinity between the two high tunneling density surfaces discussed above, electron transfer between the light-oxidized $BChl_2$ and the ferro heme *c* is drastically impeded. The basis of the binding affinity is dominated by an electrostatic interaction between complementary charges on each surface. The principal characteristic of the coulombic interaction is identified in this study as the product of the attractive force between an integrated sets of charges, seen as various negative patches on the reaction center and positive patches on the cytochrome. Of considerable interest in this work is the finding that the electron transfer rate could vary by over 10-fold among different cytochromes dictated by the different patterns of positive charges around the heme cleft. This is a much softer view of charge matching than that drawn from an expectation of one-on-one positive–negative charge matching on the surfaces and suggests that many binding positions between the two proteins may promote successful electron transfer. An envelope of rates may be expected, weighted by the distribution of positions of heme and $BChl_2$ on the cytochrome–reaction center encounter surface.

Another and quite different view of the water-exposed surface of the reaction center is that on the other, cytoplasmic side of the membrane. This area is dominated by the H subunit, which caps the Q_A and Q_B quinone binding sites but is free of any redox cofactors itself. Examination of the tunneling density at the surface emanating from either of these sites (not shown) reveals an area of protein surface some 20 Å

away that has the potential to effectively insulate against the leakage of electrons to the exterior of the reaction center from the highly reactive semiquinones. If an adventitious electron acceptor encountered and bound to the H subunit surface, then electron transfer rates could be between 10^2 and 10^{-3} s^{-1}, corresponding to rates with a ΔG from 0 to λ, where λ is around 0.7 to 1.3 eV [Eq. (3)]. However, the range of actual electron loss rates through the H subunit insulation is likely to be several orders of magnitude slower than these calculated rates, as without a specific binding interaction with the protein, the loss rate will be governed by diffusion and the concentration of the adventitious acceptor. Moreover, if the adventitious acceptor is a protein, then the additional distance from its surface to the cofactor edge has to be taken into account; a typical 5 Å distance will slow the loss rate by another 1000-fold. The normal physiological turnover rate of the Q_A semiquinone state is 10^4 s^{-1}, the native rate between the Q_A and Q_B sites. Turnover of the Q_B semiquinone state could be as fast as 10^3 s^{-1}, an approximate rate for the production of hydroquinone at the Q_B site prior to diffusion into the ubiquinone pool. However, in low light conditions the lifetime of the semiquinone states could be much longer, particularly as regards the Q_B site, and hence vulnerable to loss. More quantitative work on this topic is needed, but even with the rough guidelines sketched out above it would appear that the H subunit serves as an effective insulator against electron loss and represents a dramatic contrast to the opposite surface of the reaction center that interacts with cytochrome *c*.

Interprotein electron transfer introduces more demands than intraprotein electron transfer when it comes to experimental acquisition of the nuclear, Franck–Condon terms and the electronic terms. These demands have been nicely met in measurements of electron transfer from ferro heme of cytochrome *c* and the flash-oxidized $BChl_2$ of the reaction center (Lin *et al.*, 1994b). Free energy was changed by H-bond manipulations to the $BChl_2$ without affecting the fully formed cytochrome–reaction center complex at the time of flash activation. The ΔG-rate relationship (Fig. 2) permits a reasonable estimate of λ of 600 meV and the Franck–Condon optimized rate. This rate plotted against the edge-to-edge distance range obtained from the two cytochrome *c*-reaction center models (Allen *et al.*, 1987; Tiede and Dutton, 1993) is close to the rate distance line adhered to by the intraprotein electron transfers of the reaction center (Fig. 3). Current work on reaction center and cytochrome *c* co-crystal structures may reveal other possible positions (G. Feher, personal communication). Nevertheless, from the information available at present, it appears that the rate observed is similar to that estimated for the analogous electron transfer between cytochrome c_{559} and the $BChl_2$ of *Rp. viridis* where the cytochrome is strongly integrated into the reaction center structure (see Fig. 3). The rate also fits close along the rate–distance relationship that includes the other intraprotein electron transfers of the reaction centers, which suggests that the character of the electronic tunneling barriers medium between the $BChl_2$ and the electrostatically bound heme of *Rb. sphaeroides* is similar to the rest of the reaction center protein.

Lactate dehydrogenase (introduced in Fig. 1) presents an analogous design for electron transfer between the flavin domain and the heme *b* (b_2) domain. These domains are linked by a flexible hinge that serves to bring the faces of each domain together. The hinge evidently replaces electrostatic forces dominant in the reaction center–cytochrome *c* interaction in guiding association of the flavin and heme domains. Breaking the hinge by site-directed mutagenesis eliminates interdomain electron transfer (Sharp *et al.*, 1994). Opening up the hinge reveals that the exposed surface on each domain displays a surface of high electron tunneling density emanating from the heme and the flavin to the surface of the respective domains, a picture analogous to the reaction center and cytochrome *c*. Similarly, in each case, the cofactor is partly visible from the surface and again there is a substantial matching area for the promotion of interdomain electron transfer.

Interprotein electron transfer between the heme *b* and the external cytochrome *c* also appears analogous, although the interaction of cytochrome *c* with the heme domain is less clear than with the reaction center. Several binding models have been considered, taking into account evidence of stoichiometry, biochemical interactions, and proximities of the modeled b_2 heme to the cytochrome *c* heme (Tegoni *et al.*, 1993). Structural features in the intervening medium have also been examined in light of possible preferred pathways to enhance the electron transfer rates (Tegoni *et al.*, 1993). Our analysis of the electron tunneling density over the whole tetrameric surface reveals that insulation from unintended redox reactions is provided by the tetrameric association itself and by protein bulk in other areas. The distance between cofactors in different monomers is large, on the order of 40 Å, with the estimated electron transfer rates between monomers

[for example, using Eq. (3)] likely to be insignificant. The entire surface of the tetramer viewed from below (the lower half of the outline in Fig. 1) displays no regions of significant electron tunneling density. The lower surface also has no regions of negative charge that would attract cytochrome *c* binding; yet the top of the tetramer extending out to the end of the heme *b* (b_2) domain exhibited extensive relatively weak negative charge and hence would attract cytochrome *c* (Tegoni *et al.*, 1993). However, we find that only in the interface region between the flavin domain and the heme *b* (b_2) domain is there extensive electron tunneling density. In particular, there is a broad band of high tunneling density along this interface, extending from the top to the sides of the tetramer. The bound cytochrome *c* position shown in Fig. 1, and identified functionally most likely (Tegoni *et al.*, 1993), is located at one end of this region, but other geometries could also be redox active, perhaps recruiting cytochromes from a nearby pool attracted to the upper negative surface.

Overall, these examples support the view that electron transfer between protein complexes extends the relatively simple relationship between rate, edge-to-edge distance between cofactors, free energy, and reorganization energy that appears generally applicable to physiological intraprotein electron transfer. Complex formation is a crucial preparation for interprotein electron transfer, but relatively broad areas defining "soft" multiple binding geometries and sampling different structures of the medium between the redox centers appear to bring redox centers close enough to be physiologically productive.

REFERENCES

Allen, J. P., Feher, G., Yeates, T. O., Komiya, H., and Rees, D. C. (1987). *Proc. Natl. Acad. Sci. USA* **84**, 5725–5729.

Beitz, J. V., and Miller, J. R. (1979). In *Tunneling in Biological Systems* (Chance, B., De Vault, D. C., Frauenfelder, H., Marcus, R. A., Schrieffer, J. R., and Sutin, N., eds.), Academic Press, New York.

Beratan, D. N., Onuchic, J. N., Winkler, J. R., and Gray, H. B. (1992) *Science* **258**, 1740–1741.

Betts, J. N., Beratan, D. N., and Onuchic, J. N. (1992). *J. Am. Chem. Soc.* **114**, 4043–4046.

Casimiro, D. R., Richards, J. H., Winkler, J. R. and Gray, H. B. (1993a) *J. Phys. Chem.* **97**, 13073–13077.

Casimiro, D. R., Wong, L. L., Colon, J. L., Zewert, T. E., Richards, J. H., Chang, I. J., Winkler, J. R. and Gray, H. B. (1993b). *J. Am. Chem. Soc.* **115**, 1485–1489.

Cha, Y., Murray, C. J., and Klinman, J. P. (1989). *Science* **243**, 1325–1330.

Chang, C. H., Tiede, D., Tang, J., Smith, U., Norris, J., and Schiffer, M. (1986). *FEBS Lett.* **205**, 82–6.

Chapman, S. K., White, S. A., and Reid, G. A. (1991). *Adv. Inorg. Chem.* **36**, 257–301.

Chidsey, C. E. D., Kirmaier, C., Holten, D., and Boxer, S. G. (1985). *Biochim. Biophys. Acta* **766**, 424–437.

Devault, D. (1980). *Q. Rev. Biophys.* **13**, 387–564.

Devault, D., and Chance, B. (1966). *Biophys. J.* **6**, 825–847.

Dutton, P. L., and Moser, C. C. (1994). *Proc. Natl. Acad. Sci. USA* **91**, 10247–10250.

Edwards (1994). *Biochemistry and Physiology of the Neutrophil*, Cambridge University Press, Cambridge.

Ermler, U., Fritzsch, G., Buchanan, S. K., and Michel, H. (1994). *Structure* **2**, 925–936.

Evenson, J. W., and Karplus, M. (1993). *Science* **262**, 1247–1249.

Farid, R. S., Moser, C. C., and Dutton, P. L. (1993). *Curr. Opin. Struct. Biol.* **3**, 225–233.

Farver, O., and Pecht, I. (1992). *J. Am. Chem. Soc.* **114**, 5764–5767.

Franzen, S., Goldstein, R. F., and Boxer, S. G. (1990). *J. Phys. Chem.* **94**, 5135–5149.

Friesner, R. A., and Monge, A. (1994). *Structure* **2**, 339–43.

Giangiacomo, K. M., and Dutton, P. L. (1989). *Proc. Natl. Acad. Sci. USA* **86**, 2658–2662.

Gruschus, J. M., and Kuki, A. (1993). *J. Phys. Chem.* **97**, 5581–5593.

Gunner, M. R., and Dutton, P. L. (1989). *J. Am. Chem. Soc.* **111**, 3400–3412.

Gunner, M. R., Robertson, D. E., and Dutton, P. L. (1986). *J. Phys. Chem.* **90**, 3783–3795.

Holten, D., Windsor, M. W., Parson, W. W., and Thornber, J. P. (1978). *Biochim. Biophys. Acta* **501**, 112–126.

Holzapfel, W., Finkele, U., Kaiser, W., Oesterhelt, D., Scheer, H., Stilz, H. U., and Zinth, W. (1990). *Proc. Natl. Acad. Sci. USA* **87**, 5168–5172.

Hopfield, J. J. (1974). *Proc. Natl. Acad. Sci. USA* **71**, 3640–4.

Jia, Y. W., Dimagno, T. J., Chan, C. K., Wang, Z. Y., Du, M., Hanson, D. K., Schiffer, M., Norris, J. R., Fleming, G. R., and Popov, M. S. (1993). *J. Phys. Chem.* **97**, 13180–13191.

Jortner, J. (1976). *J. Chem. Phys.* **64**, 4860–4867.

Karpishin, T. B., Grinstaff, M. W., Komarpanicucci, S., McLendon, G., and Gray, H. B. (1994). *Structure* **2**, 415–422.

Kuki, A., and Wolynes, P. G. (1987). *Science* **236**, 1647–52.

Labahn, A., Paddock, M. L., McPherson, P. H., Okamura, M. Y., and Feher, G. (1994). *J. Chem. Phys.* **98**, 3417–3423.

Levich, V. G., and Dogonadze, R. R. (1959). *Dokl. Akad. Nauk SSSR* **124**, 123–6.

Lin, X., Murchison, H. A., Nagarajan, V., Parson, W. W., Allen, J. P., and Williams, J. C. (1994a). *Proc. Natl. Acad. Sci. USA* **91**, 10265–10269.

Lin, X., Williams, J. C., Allen, J. P., and Mathis, P. (1994b). *Biochemistry* **33**, 13517–13523.

Marcus, R. A. (1956). *J. Chem. Phys.* **24**, 966–978.

Marcus, R. A., and Sutin, N. (1985). *Biochim. Biophys. Acta* **811**, 265–322.

McLendon, G., Zhang, Q., Wallin, S. A., Miller, R. M., Billstone, V., Spears, K. G., and Hoffman, B. M. (1993). *J. Am. Chem. Soc.* **115**, 3665–3669.

Michel, H., Deisenhofer, J., and Epp, O. (1986). *EMBO J.* **5**, 2445–2451.

Miller, J. R., Beitz, J. V., and Huddleston, R. K. (1984). *J. Am. Chem. Soc.* **106**, 5057–5068.

Mitchell, P. (1961). *Nature (London)* **191**, 144–148.

Moser, C. C., and Dutton, P. L. (1992). *Biochim. Biophys. Acta* **1101**, 171–176.

Moser, C. C., Keske, J. M., Warncke, K., Farid, R. S. and Dutton, P. L. (1992). *Nature (London)* **355**, 796–802.

Moser, C. C., Sension, R. J., Szarka, A. Z., Repinec, S. T., Hochstrasser, R. M., and Dutton, P. L. (1995). *J. Chem. Phys.*, in press.

Ohnishi, S. T., and Ohnishi, T., Eds. (1993). *Cellular Membrane, A Key to Disease Processes*, CRC Press, Boca Raton.

Okamura, M. Y., and Feher, G. (1992). *Annu. Rev. Biochem.* **61**, 861–96.
Onuchic, J. N., Beratan, D. N., Winkler, J. R., and Gray, H. B. (1992). *Annu. Rev. Biophys. Biomol. Struct.* **21**, 349–77.
Padmanaban, G., Venkateswar, V., and Rangarajan, P. N. (1989). *Trends Bio. Sci.* **14**, 492.
Pan, L. P., Durham, B., Wolinska, J., and Millett, F. (1988). *Biochemistry* **27**, 7180–7184.
Parson, W. W., Clayton, R. K., and Cogdell, R. J. (1975). *Biochim. Biophys. Acta* **387**, 265–277.
Parson, W. W., Chu, Z. T., and Warshel, A. (1990). *Biochim. Biophys. Acta* **1017**, 251–72.
Pelletier, H., and Kraut, J. (1992). *Science* **258**, 1748–1755.
Schenck, C. C., Blankenship, R. E., and Parson, W. W. (1982). *Biochim. Biophys. Acta* **680**, 44–59.
Sharp, R. E., White, P., Chapman, S. K., and Reid, G. A. (1994). *Biochemistry* **33**, 5515–5120.
Shopes, R. J., and Wraight, C. A. (1985). *Biochim. Biophys. Acta* **806**, 348–356.
Siddarth, P., and Marcus, R. A. (1993). *J. Phys. Chem.* **97**, 2400–2405.
Stryer, L. (1995). *Biochemistry*, W. H. Freeman, New York.
Tegoni, M., White, S. A., Roussel, A., Mathews, F. S., and Cambillau, C. (1993). *Proteins: Struct. Funct. Gen.* **16**, 408–422.
Tiede, D. M., and Dutton, P. L. (1993). In *The Photosynthetic Bacteria* (Deisenhofer, J. and Norris, J. R., eds.), Academic Press, New York, pp. 257–288.
Tiede, D. M., Vashishta, A.-C., and Gunner, M. R. (1993). *Biochemistry* **32**, 4515–4531.
Voet, D., and Voet, J. G. (1995). *Biochemistry*, Wiley, New York.
Volk, M., Haberle, T., Feick, R., Ogrodnik, A., and Michel-Beyerle, M.-E. (1993). *J. Phys. Chem.* **97**, 9831–9836.
Warncke, K., Gunner, M. R., Braun, B. S., Gu, L., Yu, C.-A., Bruce, J. M., and Dutton, P. L. (1994). *Biochemistry* **33**, 7830–41.
Warshel, A. and Weiss, R. (1978). In *Frontiers of Biological Energetics* (Dutton, P. L., Leigh, J., and Scarpa, A. eds.), Academic Press, New York, pp. 30–36.
Warshel, A., Chu, Z. T., and Parson, W. W. (1989). *Science* **246**, 112–6.
Warshel, A., Chu, Z. T., and Parson, W. W. (1994). *J. Photochem. Photobiol.* **82**, 123–128.
Willie, A., Stayton, P. S., Sligar, S. G., Durham, B., and Millett, F. (1992). *Biochemistry* **32**, 7237–7242.
Wuttke, D. S., Bjerrum, M. J., Winkler, J. R., and Gray, H. B. (1992a). *Science* **256**, 1007–1009.
Wuttke, D. S., Bjerrum, M. J., Chang, I., Winkler, J. R., and Gray, H. B. (1992b). *Biochim. Biophys. Acta* **1101**, 168–170.
Xia, Z. X., and Mathews, F. S. (1990). *J. Mol. Biol.* **212**, 837–63.